Contribution from the Departments of Molecular Spectroscopy, Crystallography, and Solid State Physics, Research Institute for Materials, University of Nijmegen, Toernooiveld, 6525 ED Nijmegen, The Netherlands

# Structural, EPR, and Magnetic Studies of a Nonplanar Copper(II) Maleonitriledithiolate Complex

D. SNAATHORST, H. M. DOESBURG, J. A. A. J. PERENBOOM, and C. P. KEIJZERS*

The crystal structure of the complex $[Cu^{II}(mnt)_2]^{2-}[MB^+]_2\cdot$(acetone) $[CuC_{40}N_{10}S_6H_{36}\cdot C_3H_6O]$ is reported, where mnt = maleonitriledithiolato $(C_4N_2S_2)^{2-}$ and $MB^+$ = the methylene blue cation = 3,9-bis(dimethylamino)phenazothionium. The space group is $P\bar{1}$, with $a$ = 10.346 (3) Å, $b$ = 14.522 (3) Å, $c$ = 15.524 (5) Å, $\alpha$ = 93.69 (3)°, $\beta$ = 90.69 (2)°, $\gamma$ = 105.87 (3)°, and with $Z$ = 2. The residuals are $R$ = 4.4% and $R_w$ = 4.4% for 4235 independent reflections collected with a diffractometer using Mo K$\alpha$ radiation. The $MB^+$ cations are stacked along the $c$ axis. The $[Cu(mnt)_2]^{2-}$ anions are paired, these pairs being stacked along the $c$ axis as well. The anions have approximately $D_2$ symmetry with a dihedral angle of 47.4° between the planes of the ligands. The copper–sulfur distances range from 2.240 (2) to 2.261 (2) Å. Susceptibility measurements reveal an antiferromagnetic exchange coupling. An exchange $J$ of −2.6 cm$^{-1}$ was derived from a fit of a singlet–triplet model to the experimental data. Single-crystal EPR spectra are in accord with a triplet state of two coupled Cu(II) ions. The experimental **g**, copper hyperfine, and zero-field splitting tensors are compared with tensors which are calculated from semiemperical molecular orbital data.

## I. Introduction

Considerable interest has been focused on platelike transition-metal complexes because of their ability to form one-dimensional crystals[1-7] and $\pi$-donor–acceptor complexes.[8-10] Especially the complexes with 1,2-dithiolato ligands (mnt = maleonitriledithiolato $(C_4N_2S_2)^{2-}$ and thiete = $(C_4S_2F_6)^{2-}$) have been used for these studies because they form a large variety of complexes with transition-metal ions in various oxidation states, and their $\pi$-electron system seems to facilitate the mentioned structures. Typical examples of crystals with one-dimensional interactions are the salts of the paramagnetic ($S = {}^1/_2$) anions $[M(mnt)_2]^-$ with M = Ni, Pd, and Pt[2] and $[Cu(mnt)_2]^{2-}$.[1] Examples of donor–acceptor complexes are $Ni^{IV}(thiete)_2$ with the $\pi$ bases pyrene and perylene[8] and the thiete and mnt complexes of Ni(III) with the tropylium cation.[9,10]

We have prepared a salt of $[Cu(mnt)_2]^{2-}$ with the methylene blue ($MB^+$ = 3,9-bis(dimethylamino)phenazothionium) cation. The salt was obtained in two modifications: when prepared from DMF it had the expected stoichiometry $[Cu(mnt)_2](MB)_2$, but preparation from acetone yielded the stoichiometry $[Cu(mnt)_2](MB)_2\cdot$(acetone). The former compound shows one EPR line over the entire temperature range 4.2–300 K and, so far, the crystal quality was not good enough for X-ray examination. The EPR spectra of the latter complex are typical for an electronic triplet state and do show copper hyperfine splitting (hfs) besides the $g$ anisotropy and the zero-field splitting (section III C). The X-ray crystal structure (section III A) showed that the $[Cu(mnt)_2]^{2-}$ anions are not planar. They neither form regular stacks nor do they form donor–acceptor complexes with the $MB^+$ cations. Our investigations concentrated on the magnetic properties of this nonplanar complex (section III B, C) and on its electronic structure (section III C). The latter was investigated by semiempirical molecular orbital (MO) calculations and by comparison of the experimentally determined EPR parameters with the parameters which were calculated from the MO data.

## II. Experimental Section

**A. Preparation.** The complex $[Cu(mnt)_2]^{2-}[MB^+]_2$ precipitates upon mixing of ethanol/water solutions of $Na_2^+[Cu(mnt)_2]^{2-}$ and of $MB^+Cl^-$. Methylene blue was purchased from Merck. $Na_2^+[Cu(mnt)_2]^{2-}$ was prepared according to the literature method.[11]

Shiny, copper red crystals were obtained by recrystallization from dimethylformamide. The crystals have a square prismatic shape. [Anal. Calcd for $[Cu(S_2C_4N_2)_2]^{2-}(C_{16}H_{18}N_3S^+)_2$: C, 52.64; N, 15.35; H, 3.98. Found: C, 52.59; N, 15.31; H, 3.97.]

Shiny, metallic green, crystals of $[Cu(mnt)_2]^{2-}(MB^+)_2\cdot$(acetone) were obtained by recrystallization of $[Cu(mnt)_2]^{2-}(MB^+)_2$ from acetone. The crystals were found to be air-stable; no loss of acetone was detected. The shape of these crystals is octahedral. [Anal. Calcd for $[Cu(S_2C_4N_2)_2]^{2-}C_{16}H_{18}N_3S^+)_2\cdot C_3H_6O$: C, 53.20; N, 14.43; H, 4.29. Found: C, 52.72; N, 14.16; H, 4.36.]

**B. Structure Determination. 1. Collection and Reduction of Crystallographic Data.** Crystallographic data of a crystal of 0.42 × 0.20 × 0.20 mm were collected on a single-crystal CAD4 diffractometer using Mo K$\alpha$ radiation ($\lambda$ = 0.710 69 Å), monochromated with a graphite crystal monochromator. The unit cell dimensions were calculated from the setting angles of 25 reflections having 38° < 2$\theta$ < 42°. The lattice constants are $a$ = 10.346 (3) Å, $b$ = 14.522 (3) Å, $c$ = 15.524 (5) Å, $\alpha$ = 93.69 (3)°, $\beta$ = 90.69 (2)°, $\gamma$ = 105.87 (3)°, and $V$ = 2237.6 Å$^3$ of space group $P\bar{1}$, with $\rho$(calcd) = 1.441 g cm$^{-3}$, $\rho$(obsd) = 1.430 g cm$^{-3}$ (flotation method in a benzene/tetrachloromethane mixture), $Z$ = 2, linear absorption coefficient $\mu$(Mo K$\alpha$) = 8.25 cm$^{-1}$. The data were collected in the $\omega$–2$\theta$ scan mode at a variable scan speed, with a maximum of 40 s/reflection. A total of 15722 reflections having 2° < $\theta$ < 25° were recorded ($\pm h$, $\pm k$, $\pm l$). Three standard reflections were measured after every 1800 s of X-ray exposure, and it was observed that the intensity remained constant within 1%.

After equivalent reflections ($R_{av}$ [=$[(\sum||I| - |\bar{I}||)/\sum|I|]$] = 0.023 including all reflections) were averaged, 7861 reflections remained of which 3626 had $I < 3\sigma(I)$ ($\sigma(I)$ based on counting statistics). Comparison of the falloff of "unobserved" reflections with $(\sin\theta)/\lambda$ and the falloff of observed reflections led to the deletion of 3120 unobserved reflections and a considerable saving of time during the least-squares refinement. The intensity data of the remaining 4741 reflections were corrected for Lorentz and polarization effects and then reduced to $|F_o|$ values. Correction of the data for absorption was not considered to be necessary.

**2. Solution and Refinement of the Structure.** The phase problem was solved by use of the MULTAN[12] program, with the use of the 400

* To whom correspondence should be addressed at the Department of Molecular Spectroscopy.

(1) Plumlee, K. W.; Hoffman, B. M.; Ibers, J. A.; Soos, Z. G. *J. Chem. Phys.* **1975**, *63*, 1926.
(2) Maki, A. H.; Edelstein, N.; Davidson, A.; Holm, R. H. *J. Am. Chem. Soc.* **1964**, *86*, 4580.
(3) Plumlee, K. W.; Hoffman, B. M.; Ratjack, M. T.; Kannewurf, C. R. *Solid State Commun.* **1974**, *15*, 1651.
(4) Alcacev, L.; Maki, A. H. *J. Chem. Phys.* **1974**, *78*, 215.
(5) Wudl, F.; Ho, C. H.; Nagel, A. *J. Chem. Soc., Chem. Commun.* **1973**, 923.
(6) Interrante, L. V.; Browall, K. W.; Hart, H. R.; Jacobs, I. S.; Watkins, G. D.; Wee, S. H. *J. Am. Chem. Soc.*, **1975**, *97*, 889.
(7) Jacobs, I. S.; Bray, J. W.; Hart, H. R.; Interrante, L. V.; Kasper, J. S.; Watkins, G. D.; Prober, D. E.; Bonner, J. C. *Phys. Rev. B: Solid State* **1976**, *B14*, 3036.
(8) Schmidt, R. D.; Wing, R. M.; Maki, A. H. *J. Am. Chem. Soc.* **1969**, *91*, 4391.
(9) Wing, R. M.; Schlupp, R. L. *Inorg. Chem.* **1970**, *9*, 471.
(10) Manoharan, P. T.; Noordik, J. H.; de Boer, E.; Keijzers, C. P. *J. Chem. Phys.* **1981**, *74*, 1980.
(11) Davidson, A.; Holm, R. H. *Inorg. Synth.* **1971**, *10*, 8.

0020-1669/81/1320-2526$01.25/0 

Table I. Fractional Positional Coordinates[a]

| atom | x | y | z |
|---|---|---|---|
| Cu | 0.4852 (1) | 0.3494 (1) | 0.6736 (1) |
| S(1) | 0.4949 (1) | 0.2661 (1) | 0.5491 (1) |
| S(2) | 0.3718 (1) | 0.4630 (1) | 0.5958 (1) |
| S(3) | 0.5985 (2) | 0.4362 (1) | 0.7966 (1) |
| S(4) | 0.4712 (1) | 0.2266 (1) | 0.7533 (1) |
| S(5) | −0.1396 (1) | −0.0323 (1) | 0.3377 (1) |
| S(6) | −0.2565 (1) | 0.0023 (1) | 0.0832 (1) |
| N(1) | 0.3668 (5) | 0.2723 (4) | 0.3042 (3) |
| N(2) | 0.2086 (5) | 0.5074 (4) | 0.3605 (4) |
| N(3) | 0.7406 (6) | 0.4179 (4) | 1.0365 (4) |
| N(4) | 0.5472 (5) | 0.1704 (4) | 0.9882 (3) |
| N(5) | 0.1742 (4) | −0.0215 (3) | 0.3860 (3) |
| N(6) | 0.0576 (4) | 0.0097 (3) | 0.1399 (3) |
| N(7) | −0.0594 (4) | 0.2828 (3) | 0.5040 (3) |
| N(8) | −0.0656 (4) | −0.3403 (3) | 0.1902 (3) |
| N(9) | −0.1801 (5) | 0.3170 (3) | 0.2506 (3) |
| N(10) | −0.1838 (5) | −0.3059 (3) | −0.0627 (3) |
| C(1) | 0.4058 (5) | 0.3358 (3) | 0.4673 (3) |
| C(2) | 0.3562 (5) | 0.4178 (4) | 0.4879 (4) |
| C(3) | 0.6050 (5) | 0.3600 (4) | 0.8787 (4) |
| C(4) | 0.5499 (5) | 0.2726 (3) | 0.8601 (3) |
| C(5) | 0.3846 (5) | 0.3011 (4) | 0.3764 (4) |
| C(6) | 0.2775 (5) | 0.4687 (4) | 0.4162 (4) |
| C(7) | 0.6779 (6) | 0.3922 (4) | 0.9676 (4) |
| C(8) | 0.5525 (5) | 0.2157 (4) | 0.9324 (4) |
| C(9) | 0.0164 (6) | −0.4099 (4) | 0.1613 (4) |
| C(10) | −0.2101 (6) | −0.3591 (4) | 0.1663 (4) |
| C(11) | −0.0103 (5) | −0.2612 (3) | 0.2377 (3) |
| C(12) | −0.0891 (4) | −0.1940 (3) | 0.2640 (3) |
| C(13) | −0.0335 (4) | −0.1138 (3) | 0.3114 (3) |
| C(14) | 0.1102 (5) | −0.0972 (3) | 0.3383 (3) |
| C(15) | 0.1881 (5) | −0.1667 (4) | 0.3118 (4) |
| C(16) | 0.1337 (5) | −0.2458 (4) | 0.2646 (4) |
| C(17) | −0.0319 (4) | 0.0559 (3) | 0.3975 (3) |
| C(18) | 0.1111 (5) | 0.0486 (3) | 0.4133 (3) |
| C(19) | 0.1908 (5) | 0.1251 (3) | 0.4633 (3) |
| C(20) | 0.1365 (5) | 0.1998 (3) | 0.4934 (3) |
| C(21) | −0.0053 (5) | 0.2070 (3) | 0.4756 (3) |
| C(22) | −0.0889 (5) | 0.1324 (3) | 0.4270 (3) |
| C(23) | −0.2047 (5) | 0.2917 (4) | 0.4872 (4) |
| C(24) | 0.0204 (6) | 0.3612 (4) | 0.5535 (4) |
| C(25) | −0.3294 (6) | −0.3195 (4) | −0.0900 (4) |
| C(26) | −0.1067 (7) | −0.3793 (4) | −0.0922 (4) |
| C(27) | −0.1280 (5) | −0.2278 (3) | −0.0150 (3) |
| C(28) | −0.2059 (5) | −0.1589 (4) | 0.0092 (4) |
| C(29) | −0.1489 (5) | −0.0792 (3) | 0.0593 (3) |
| C(30) | −0.0066 (5) | −0.0645 (3) | 0.0897 (3) |
| C(31) | 0.0724 (5) | −0.1350 (4) | 0.0650 (4) |
| C(32) | 0.0162 (5) | −0.2135 (4) | 0.0136 (4) |
| C(33) | −0.1490 (5) | 0.0899 (3) | 0.1447 (3) |
| C(34) | −0.0062 (5) | 0.0806 (3) | 0.1646 (3) |
| C(35) | 0.0731 (5) | 0.1566 (4) | 0.2172 (4) |
| C(36) | 0.0179 (5) | 0.2327 (4) | 0.2454 (4) |
| C(37) | −0.1252 (5) | 0.2411 (3) | 0.2238 (3) |
| C(38) | −0.2059 (5) | 0.1667 (3) | 0.1728 (3) |
| C(39) | −0.0966 (7) | 0.3964 (4) | 0.2985 (5) |
| C(40) | −0.3260 (6) | 0.3276 (4) | 0.2236 (5) |
| C(41) | 0.5697 (7) | 0.9675 (6) | 0.7909 (6) |
| C(42) | 0.4755 (5) | 0.9362 (4) | 0.7063 (5) |
| C(43) | 0.4872 (8) | 0.9781 (6) | 0.6255 (6) |
| O | 0.3902 (4) | 0.8787 (3) | 0.7018 (3) |

[a] Standard deviation in the last digit is in parentheses.

highest $E$ values. The $E$ values were calculated with the Debye curve via the $K$ curve method. From the $E$ map with the highest figure of merit, the positions of two complete methylene blue cations and nine atoms of the $[Cu(mnt)_2]^{2-}$ anion could be deduced. The remaining nonhydrogen atoms were located with the use of standard difference Fourier techniques. A block-diagonal least-squares refinement (weighting scheme $w = [\sigma_c^2 + 0.0011F_o^2]^{-1}$) using 4235 reflections with $I > 3\sigma(I)$ and subsequent difference Fourier analyses resulted in the determination of 34 H atoms. The positional parameters of the remaining eight H atoms were calculated. All hydrogen atoms were assigned a fixed isotropic temperature factor of 4.4 Å$^2$. Final refinement of positional parameters and anisotropic temperature factors converged to an $R$ value [$=\sum(|F_o| - |F_c|)/\sum|F_o|$] of 0.044 and $R_w$ [$=[\sum w(|F_o| - |F_c|)^2/w|F_o|^2]^{1/2}$] = 0.044. A final difference Fourier map showed a residual electron density of 0.68 e/Å$^3$ near Cu. Other peaks were below 0.4 e/Å$^3$. The atomic scattering factors used for Cu, S, N, C, and O were taken from Cromer and Mann[13] and for H from Stewart et al.[14] No anomalous scattering factors for Cu and S were used. All crystallographic calculations were executed with use of the XRAY-72 program.[15] Positional parameters are listed in Tables I and II[16] bond distances and angles in Tables III and IV. The numbering of the atoms is shown in Figure 1. Observed and calculated structure factors are available.[16] Anisotropic temperature factors of the nonhydrogen atoms are listed in Table V.[16]

(12) Main, P. MULTAN 78, 1978.

Table III. $[Cu(mnt)_2]^{2-}$ Bond Distances (Å) and Angles (Deg)[a]

| | | | |
|---|---|---|---|
| Cu–S(1) | 2.240 (2) | C(2)–C(6) | 1.440 (7) |
| Cu–S(2) | 2.255 (2) | C(3)–C(7) | 1.425 (7) |
| Cu–S(3) | 2.245 (2) | C(4)–C(8) | 1.431 (7) |
| Cu–S(4) | 2.261 (2) | C(1)–C(2) | 1.356 (7) |
| S(1)–C(1) | 1.742 (5) | C(3)–C(4) | 1.366 (7) |
| S(2)–C(2) | 1.724 (6) | C(5)–N(1) | 1.136 (7) |
| S(3)–C(3) | 1.730 (6) | C(6)–N(2) | 1.143 (7) |
| S(4)–C(4) | 1.721 (5) | C(7)–N(3) | 1.126 (7) |
| C(1)–C(5) | 1.425 (7) | C(8)–N(4) | 1.133 (7) |
| S(1)–Cu–S(2) | 93.1 (2) | S(3)–C(3)–C(4) | 122.8 (4) |
| S(1)–Cu–S(4) | 95.5 (2) | S(3)–C(3)–C(7) | 115.8 (4) |
| S(2)–Cu–S(3) | 98.1 (2) | S(4)–C(4)–C(3) | 123.7 (4) |
| S(3)–Cu–S(4) | 92.6 (2) | S(4)–C(4)–C(8) | 117.0 (3) |
| Cu–S(1)–C(1) | 100.3 (3) | C(2)–C(1)–C(5) | 121.1 (4) |
| Cu–S(2)–C(2) | 99.8 (3) | C(1)–C(2)–C(6) | 118.9 (4) |
| Cu–S(3)–C(3) | 100.7 (3) | C(4)–C(3)–C(7) | 121.3 (4) |
| Cu–S(4)–C(4) | 100.2 (3) | C(3)–C(4)–C(8) | 119.4 (4) |
| S(1)–C(1)–C(2) | 122.5 (4) | C(1)–C(5)–N(1) | 179.0 (12) |
| S(1)–C(1)–C(5) | 116.3 (4) | C(2)–C(6)–N(2) | 176.1 (6) |
| S(2)–C(2)–C(1) | 124.2 (4) | C(3)–C(7)–N(3) | 176.9 (7) |
| S(2)–C(2)–C(6) | 116.7 (4) | C(4)–C(8)–N(4) | 176.3 (6) |

[a] Standard deviation in last digit is in parentheses.

**C. Magnetization Measurements.** The magnetic moment of a powdered sample was determined at a field of 0.814 T with a very sensitive magnetometer with the use of a superconducting set of pickup coils[17] and a very low frequency sample position modulation.[18] In the superconducting circuit, two oppositely wound pickup coils are positioned coaxially with the magnetic field generated by a superconductive solenoid. With the present coil geometry, a shielding current will flow in this circuit which is linearly proportional to the position of the sample over a range of several millimeters. The current is measured with a fluxgated galvanometer of similar design as reported by Poerschke and Wollenberger.[18,19] The relevant low-frequency modulation at the output of the galvanometer is detected with common lock-in techniques. The output voltage of the instrument is proportional to the magnetic moment of the sample up to a moment of $0.5 \times 10^{-3}$ J/T. The instrument was calibrated against the saturation magnetization of a small nickel sample; the accuracy of the calibration is in order of 1%. The noise corresponds with $\Delta m = 3 \times 10^{-9}$ J/T ($3 \times 10^{-6}$ emu) when the magnet is operated in its persistent mode. A continuous-flow cryostat is inserted through the pickup coils and allows regulation of sample temperature between 2.5 and 300 K. The temperature is determined from a carbon-resistance thermometer fixed to the wall of the cryostate, close to the sample. The resistance thermometer was calibrated in situ against a factory calibrated germanium thermometer. Below 100 K the precision of the temperature determination is better than 1%. Above 100 K the sample

(13) Cromer, D.; Mann, J. *Acta Crystallogr., Sect. A* **1968**, *A24*, 321.
(14) Stewart, R. F.; Davidson, E. R.; Simpson, W. T. *J. Chem. Phys.* **1965**, *42*, 3175.
(15) "The X-ray System" (version of June 1972), Technical Report TR-192; Computer Science Center, University of Maryland: College Park, MD, June 1972.
(16) Supplementary material.
(17) Gelsing, R. R.; van Kempen, H. *Proc. Int. Cryog. Eng. Conf.* **1970**, *4*, 233.
(18) Van Kempen, H.; Perenboom, J. A. A. J.; Wyder, P., to be submitted for publication.
(19) Poerschke, R.; Wollenberger, H. *Cryogenics* **1976**, *10*, 333.

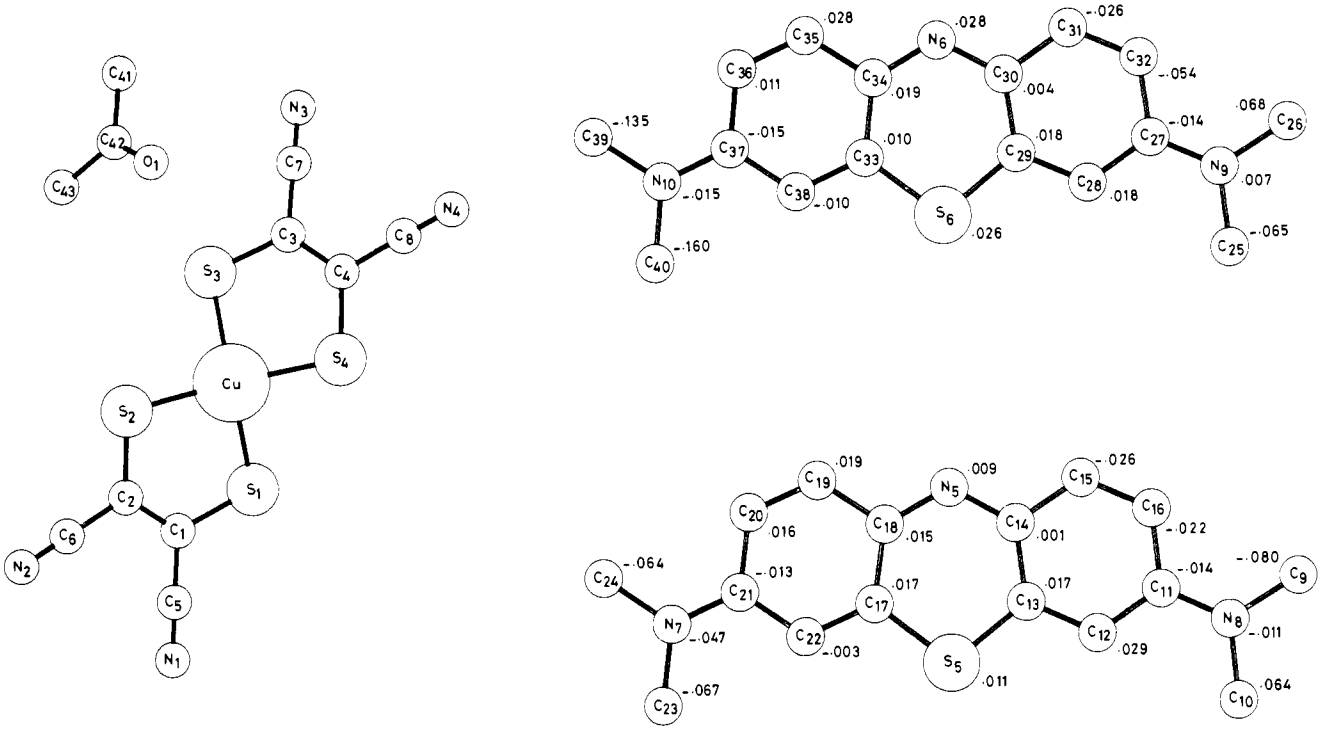


**Figure 1.** Atomic numbering of the crystallographic asymmetric unit. Individual atomic deviations (in Å) from the best planes of the methylene blue cations are also given.

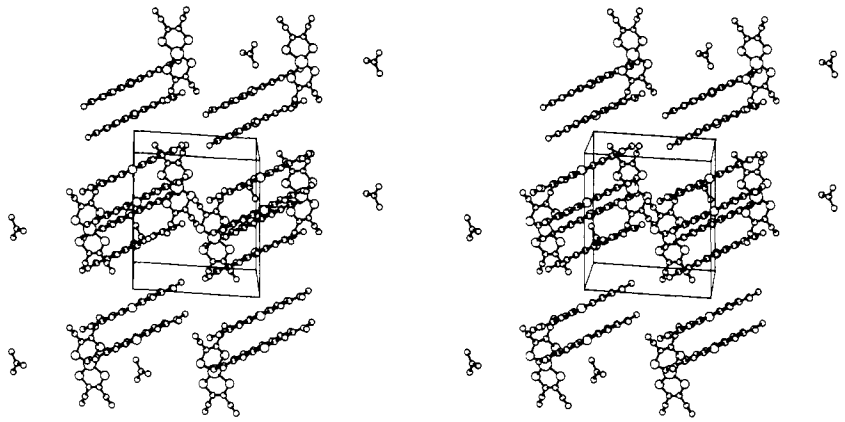

**Figure 2.** Stereoview of the packing as viewed along the *a* axis. Only half of the $MB^+$ cations are shown; the other half are generated by the inversion center at (0, 0, 0) (see text).

temperature is determined from the voltage of a Au(0.03% Fe)–chromel thermocouple linked to the temperature-regulated diffusor, a few centimeters below the sample.

**D. EPR Measurements.** The EPR measurements were carried out at 4.2 K on a Varian E-12 X-band spectrometer, with the use of an Oxford Instruments BKESR12 flow cryostat. The microwave frequency was measured with a HP 5246L counter, equipped with a 5255A plug-in unit. The dc magnetic field was measured with a Bruker B-NM12 gaussmeter. The spectra were recorded in three orthogonal but arbitrary planes with intervals of 10° of rotation. The orientation of the crystal axes with respect to the three rotation axes was determined with a CAD4 X-ray diffractometer at room temperature. In this way, the measured EPR parameters could be transformed from the rotation axes to the crystal axes system, assuming that there are no significant structural changes upon cooling to liquid-helium temperature.

## III. Results and Discussion

**A. Crystal Structure.** A projection of the structure, as viewed along the *a* axis, is presented in Figure 2. The figure shows that the crystal contains regular stacks of $MB^+$ cations along the *c* axis and pairs of $[Cu(mnt)_2]^{2-}$ anions. The molecules in the latter are related to each other via the inversion center at (0.5, 0.5, 0.5). The Cu–Cu distance is 7.115 (1) Å, but the distance between the least-squares planes of overlapping Cu–mnt pairs is 3.82 Å and the shortest intermolecular atom–atom distance is 3.67 Å (between S(3) and N(2)). Since the $[Cu(mnt)_2]^{2-}$ pairs are separated from each other by the $MB^+$ cations in the *a* direction (Figure 3) and by the acetone molecules in the *b* direction (Figure 2), the pairs

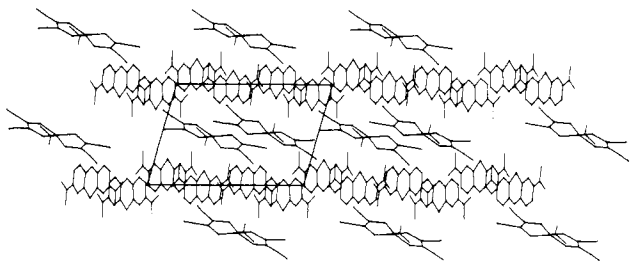

**Figure 3.** Projection of the packing arrangement. The unit cell is oriented with the $+c$ axis horizontal, the $+a$ axis vertical, and the $+b$ axis pointing toward the reader.

**Table IV.** Bond Distances (Å) and Angles (Deg) of the Two Methylene Blue Cations and the Acetone Molecule

Bond Distances

| | | | |
|---|---|---|---|
| N(5)–C(14) | 1.343 (5) | N(6)–C(30) | 1.342 (6) |
| N(5)–C(18) | 1.324 (6) | N(6)–C(34) | 1.322 (6) |
| S(5)–C(13) | 1.728 (5) | S(6)–C(29) | 1.726 (5) |
| S(5)–C(17) | 1.729 (4) | S(6)–C(33) | 1.731 (4) |
| N(7)–C(21) | 1.344 (6) | N(9)–C(25) | 1.456 (7) |
| N(7)–C(23) | 1.463 (7) | N(9)–C(26) | 1.462 (7) |
| N(7)–C(24) | 1.444 (6) | N(9)–C(27) | 1.345 (6) |
| N(8)–C(9) | 1.453 (7) | N(10)–C(37) | 1.340 (6) |
| N(8)–C(10) | 1.456 (7) | N(10)–C(39) | 1.464 (6) |
| N(8)–C(11) | 1.355 (6) | N(10)–C(40) | 1.465 (7) |
| C(11)–C(12) | 1.391 (7) | C(27)–C(28) | 1.389 (7) |
| C(11)–C(16) | 1.443 (7) | C(27)–C(32) | 1.444 (7) |
| C(12)–C(13) | 1.368 (6) | C(28)–C(29) | 1.382 (6) |
| C(13)–C(14) | 1.443 (6) | C(29)–C(30) | 1.426 (6) |
| C(14)–C(15) | 1.409 (7) | C(30)–C(31) | 1.416 (7) |
| C(15)–C(16) | 1.350 (7) | C(31)–C(32) | 1.374 (7) |
| C(17)–C(18) | 1.438 (6) | C(33)–C(34) | 1.434 (7) |
| C(17)–C(22) | 1.375 (6) | C(33)–C(38) | 1.369 (6) |
| C(18)–C(19) | 1.426 (6) | C(34)–C(35) | 1.433 (6) |
| C(19)–C(20) | 1.343 (7) | C(35)–C(36) | 1.352 (7) |
| C(20)–C(21) | 1.423 (7) | C(36)–C(37) | 1.434 (7) |
| C(21)–C(22) | 1.416 (6) | C(37)–C(38) | 1.413 (6) |
| C(41)–C(42) | 1.447 (8) | | |
| C(42)–C(43) | 1.462 (10) | | |
| C(42)–O | 1.192 (7) | | |

Bond Angles

| | | | |
|---|---|---|---|
| C(14)–N(5)–C(18) | 123.4 (4) | C(30)–N(6)–C(34) | 122.9 (4) |
| N(5)–C(14)–C(13) | 125.3 (4) | N(6)–C(30)–C(29) | 125.5 (4) |
| N(5)–C(14)–C(15) | 118.2 (4) | N(6)–C(30)–C(31) | 117.9 (4) |
| C(13)–C(14)–C(15) | 116.5 (4) | C(29)–C(30)–C(31) | 116.6 (4) |
| C(14)–C(15)–C(16) | 122.8 (4) | C(30)–C(31)–C(32) | 122.3 (4) |
| C(15)–C(16)–C(17) | 120.0 (5) | C(31)–C(32)–C(27) | 120.2 (5) |
| C(16)–C(11)–N(8) | 120.3 (4) | C(32)–C(27)–N(9) | 120.6 (4) |
| C(16)–C(11)–C(12) | 118.1 (4) | C(32)–C(27)–C(28) | 117.7 (4) |
| C(11)–N(8)–C(10) | 121.1 (4) | C(27)–N(9)–C(25) | 119.8 (4) |
| C(11)–N(8)–C(9) | 121.6 (4) | C(27)–N(9)–C(26) | 123.8 (4) |
| C(10)–N(8)–C(9) | 117.3 (4) | C(25)–N(9)–C(26) | 116.4 (4) |
| N(8)–C(11)–C(12) | 121.5 (4) | N(9)–C(27)–C(28) | 121.7 (5) |
| C(11)–C(12)–C(13) | 121.6 (4) | C(27)–C(28)–C(29) | 121.8 (4) |
| C(12)–C(13)–C(14) | 120.9 (4) | C(28)–C(29)–C(30) | 121.3 (4) |
| C(12)–C(13)–S(5) | 118.4 (3) | C(28)–C(29)–S(6) | 117.4 (4) |
| C(14)–C(13)–S(5) | 120.7 (3) | C(30)–C(29)–S(6) | 121.2 (3) |
| C(13)–S(5)–C(17) | 104.0 (2) | C(29)–S(6)–C(33) | 103.5 (2) |
| S(5)–C(17)–C(18) | 120.3 (3) | S(6)–C(33)–C(34) | 120.2 (4) |
| C(17)–C(18)–N(5) | 126.4 (4) | C(33)–C(34)–N(6) | 126.7 (4) |
| S(5)–C(17)–C(22) | 117.3 (3) | S(6)–C(33)–C(38) | 117.4 (4) |
| C(18)–C(17)–C(22) | 122.4 (3) | C(34)–C(33)–C(38) | 112.4 (4) |
| C(17)–C(22)–C(21) | 119.6 (4) | C(33)–C(38)–C(37) | 121.0 (4) |
| C(22)–C(21)–C(20) | 118.6 (4) | C(38)–C(37)–C(36) | 117.5 (4) |
| C(22)–C(21)–N(7) | 120.4 (4) | C(38)–C(37)–N(10) | 121.3 (4) |
| C(21)–N(7)–C(23) | 122.1 (4) | C(37)–N(10)–C(39) | 121.3 (4) |
| C(21)–N(7)–C(24) | 123.0 (4) | C(37)–N(10)–C(40) | 120.8 (4) |
| C(23)–N(7)–C(24) | 114.8 (4) | C(39)–N(10)–C(40) | 117.5 (4) |
| N(7)–C(21)–C(20) | 121.0 (4) | N(10)–C(37)–C(36) | 121.1 (4) |
| C(21)–C(20)–C(19) | 121.2 (4) | C(37)–C(36)–C(35) | 121.0 (4) |
| C(20)–C(19)–C(18) | 122.5 (14) | C(36)–C(35)–C(34) | 122.6 (4) |
| C(19)–C(18)–C(17) | 115.8 (4) | C(35)–C(34)–C(33) | 115.4 (4) |
| C(19)–C(18)–N(5) | 117.8 (4) | C(35)–C(34)–N(6) | 117.9 (4) |
| C(41)–C(42)–C(43) | 117.7 (5) | | |
| C(41)–C(42)–O | 121.8 (6) | | |
| C(43)–C(42)–O | 120.5 (5) | | |

can be considered as being stacked along the *c* axis. However, the shortest interpair Cu–Cu distance is 10.743 (1) Å. Whereas the ring atoms Cu, S, and C are involved in the *intra*pair interactions, the closest *inter*pair contacts are via the CN groups and over a much longer distance (5.15 Å between C(7) and N(3)). Therefore, the interactions in the pairs are expected to be much stronger than between the pairs.

The $MB^+$ cations are essentially planar. The distances of the atoms from the least-squares planes are shown in Figure 1. The largest deviations are found for the carbon atoms of the dimethylamino groups, these groups being rotated out of the planes by angles of 1.6–4.0°. The bond lengths in both cations are comparable to those in other methylene blue structures.[20-22] The mean separation between the $MB^+$ cations in the pairs is 3.49 Å. The cations which are shown in Figure 2 are paired in a syn orientation. Because of the inversion center at (0, 0, 0), these pairs have an anti orientation relative to the symmetry related pairs which are not shown in the figure. The distance between the pairs is 3.47 Å, so that the cations are regularly stacked.

**Table VI.** Two Least-Squares Planes for the Cu-mnt Parts of the $[Cu(mnt)_2]^{2-}$ Anion

Plane Equation: $Px + Qy + Rz + S = 0$

| | plane 1 | plane 2 | | plane 1 | plane 2 |
|---|---|---|---|---|---|
| P | 9.1384 | 9.725 | R | −3.9418 | −5.336 |
| Q | 6.6475 | −4.838 | S | −4.1138 | +0.553 |

Distance (Å) from the Plane

| atom | deviation | atom | deviation |
|---|---|---|---|
| Cu[a] | −0.012 | Cu[b] | −0.013 |
| S(1)[a] | 0.014 | S(3)[b] | 0.009 |
| S(2)[a] | 0.011 | S(4)[b] | 0.018 |
| C(1)[a] | −0.009 | C(3)[b] | 0.003 |
| C(2)[a] | −0.003 | C(4)[b] | −0.017 |
| C(5) | −0.083 | C(7) | 0.075 |
| C(6) | −0.102 | C(8) | −0.097 |
| N(1) | −0.149 | N(3) | 0.182 |
| N(2) | −0.225 | N(4) | −0.222 |

[a] Atoms which define plane 1. [b] Atoms which define plane 2.

The copper–sulfur bond distances are all different and range from 2.240 to 2.261 Å (a spread of $12\sigma$), although they are expected to be chemically equivalent. Identical situations are found in the tetrabutylammonium[1] and in the tetraethylammonium[3] mnt compounds, but those copper–sulfur distances are larger. This can be attributed to the fact that the $[Cu(mnt)_2]^{2-}$ anions in those complexes are planar, while the anion in the current system exhibits a pronounced nonplanar geometry (Figure 4) with a dihedral angle of 47.4° between the least-squares planes of the two ligands (Table VI). Nonplanarity is very uncommon in bis(1,2-dithioleno) complexes and is generally caused by dimerization via methyl–sulfur linkages. Examples are $Co_2(S_2C_2(CF_3)_2)_4$,[23] $[Co_2(S_2C_6Cl_4)_4]^{2-}$,[24] and $[Fe_2(S_2C_2(CN)_2)_4]^{2-}$,[25] in which dimers the metal atoms are displaced out of the basal planes of the molecules by about 0.3 Å. All other 1,2-dithioleno complexes are planar, including the monomeric dianionic complexes $[M(mnt)_2]^{2-}$ (M = Co,[26] Ni,[27-29] Cu[1]), the dimeric monoanionic complexes,[28,30-32] and the donor–acceptor complexes of organic donors with $[Ni(mnt)_2]^-$[10] and with $[NiS_2C_2(CF_3)_2]^{0,1-}$.[8,9]

In order to examine whether the intermolecular contacts in this specific arrangement could be responsible for the

(20) Marr, H. E.; Stewart, J. M.; Chin, M. F. *Acta Crystallogr., Sect. B* **1973**, *B29*, 847.
(21) Kalm-Harari, A.; Ballard, R. E.; Norris, E. K. *Acta Crystallogr., Sect. B* **1973**, *B29*, 1124.
(22) Endres, H.; Jeromin, G.; Keller, H. J. *Z. Naturforsch., B* **1977**, *32B*, 1375.
(23) Enemark, J. H.; Lipscomb, W. N. *Inorg. Chem.* **1965**, *4*, 1729.
(24) Baker-Hawkes, M. J.; Dori, Z.; Eisenberg, R.; Gray, H. B. *J. Am. Chem. Soc.* **1968**, *90*, 4253.
(25) Hamilton, W. C.; Bernal, I. *Inorg. Chem.* **1967**, *6*, 2003.
(26) Forrester, J. D.; Zalkin, A.; Templeton, D. H. *Inorg. Chem.* **1964**, *3*, 1500.
(27) Eisenberg, R.; Ibers, J. A. *Inorg. Chem.* **1965**, *4*, 605.
(28) Kobayashi, A.; Sasaki, Y. *Bull. Chem. Soc. Jpn.* **1977**, *50*, 2650.
(29) Hove, M. J.; Hoffman, B. M.; Ibers, J. A. *J. Chem. Phys.* **1972**, *56*, 3490.
(30) Fritchie, C. J. *Acta Crystallogr.* **1966**, *20*, 107.
(31) Forrester, J. D.; Zalkin, A.; Templeton, D. H. *Inorg. Chem.* **1964**, *3*, 1507.
(32) Enemark, J. H.; Ibers, J. A. **1968**, *Inorg. Chem. 7*, 2636.

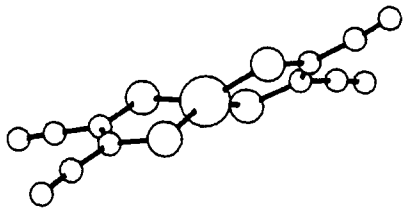

**Figure 4.** Stereoscopic view of the $[Cu(mnt)_2]^{2-}$ anion.

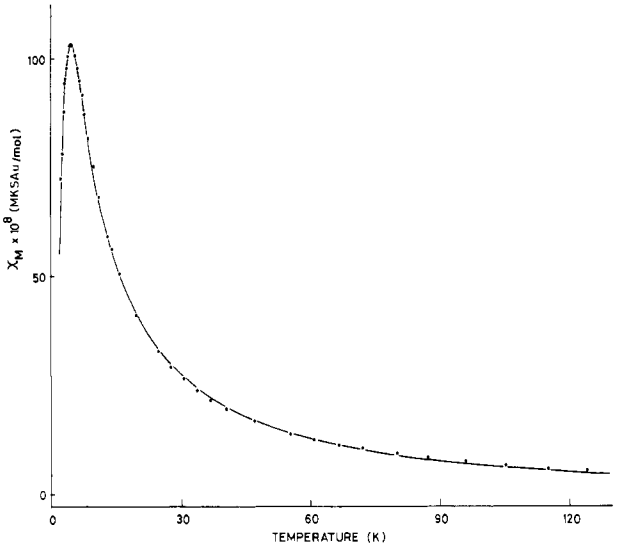


**Figure 5.** Experimental molar susceptibility data (●) per dimer. The solid line corresponds to an antiferromagnetic exchange coupling in isolated pairs.

nonplanarity of the anion, we calculated intermolecular distances for the actual structure and for a structure in which both mnt ligands were rotated over an angle of 23.7° in an opposite direction, thus yielding a planar anion. Apart from the large changes in the intrapair distances, the most striking changes are in the contacts between the anions and the hydrogen atoms of the $MB^+$ cations, e.g., H(C(31))–N(4) changes from 3.44 to 1.85 Å and H(C(40))–N(3) from 2.75 to 2.22 Å, both much less than the nonbonded contact distance as estimated from van der Waals radii. Thus, the nonplanarity of the $[Cu(mnt)_2]^{2-}$ anion can mainly be ascribed to the introduction of the large methylene blue molecules as counterions.

**B. Magnetic Susceptibility.** Figure 5 shows a plot of the molar susceptibility $\chi_M$ vs. $T$ over the temperature range 2.3–124 K. The susceptibility shows a maximum at 4.4 K, which indicates an antiferromagnetic exchange interaction. The experimental data are compared with the singlet–triplet model of two spins $S = {}^1/_2$ coupled by an isotropic exchange interaction ($\mathcal{H} = -2J\,\vec{S}_1\cdot\vec{S}_2$). In this model, the temperature dependence of the molar susceptibility is given by[33] eq 1 for

$$\chi_M(T) = (\mu_0 2N_0 g^2 \mu_B{}^2/kT)[3 + \exp(-2J/kT)]^{-1} + \chi_{cor} \quad (1)$$

a dimer, where all symbols have their usual meaning. $\chi_{cor}$ includes the diamagnetic susceptibility and the temperature-independent paramagnetism of the sample and the effective susceptibility of the sample holder. The error function (eq 2)

$$(1/N)\sum_i [\chi_{M,exptl}(T_i) - \chi_{M,calcd}(T_i)]^2 T_i^2 \quad (2)$$

was minimized by varying $J$, $g$, and $\chi_{cor}$. The exchange parameter $J$ was obtained from a fit to the data in the temperature range 3.3–9.7 K. The exchange constant $J$ was fixed when finally the fit was made to all data over the whole temperature range. The best result was obtained with $J = -2.6$ cm$^{-1}$, $g = 2.015$, and $\chi_{cor} = -25 \times 10^{-9}$ MKSA/mol ($[\chi_M{}^{MKSA}] = 4\pi \times 10^{-6}[\chi_M{}^{cgs}]$). The experimental data and the theoretical curve corresponding to eq 1 are shown in Figure 5. The deviation from the curve is for none of the points larger than 2%. The difference between the obtained $g$ value and the average value ($g^2 = (2g_\perp{}^2 + g_\parallel{}^2)/3 = 2.046^2$) from the EPR experiment is 1.5%, slightly more than the accuracy of the calibration. A possible explanation could be that the EPR $g$ value was determined for the triplet state which arises from intrapair Cu(II)–Cu(II) exchange interaction; interpair-exchange interactions which are clearly present (section III C) can possibly influence the magnetic susceptibility. The value obtained for $\chi_{cor}$ is quite reasonable, considering the measured effective susceptibility of the sample holder ($-16.5 \times 10^{-9}$ MKSA/mol), the calculated diamagnetic susceptibility of the sample[34] ($-12.0 \times 10^{-9}$ MKSA/mol), and the commonly used value of $1.5 \times 10^{-9}$ MKSA/mol for the TIP of two Cu(II) ions. Taking into account the splitting of the triplet manifold (section III C, Table VII) had no significant effect on the calculated susceptibility in the measured temperature range.

The very good correspondence between the calculated and the experimental susceptibility data indicates that the antiferromagnetic exchange interaction can be interpreted with a singlet–triplet model. As discussed in the previous section, the model of isolated pairs is also supported by the crystal structure which suggests large interactions via the overlap of the $\pi$-molecular orbitals (MO's) of the $[Cu(mnt)_2]^{2-}$ anions in the pairs and a very poor overlap between the pairs. As will be discussed in the next section, the fact that the anions are twisted, rather than planar, increases the amount of Cu $4p_z$ and S $3p_z$ character in the MO of the unpaired electron, thus enhancing this effect.

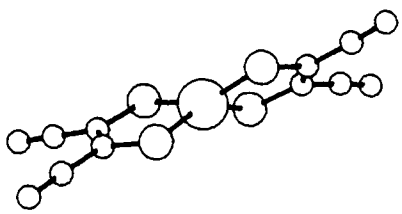

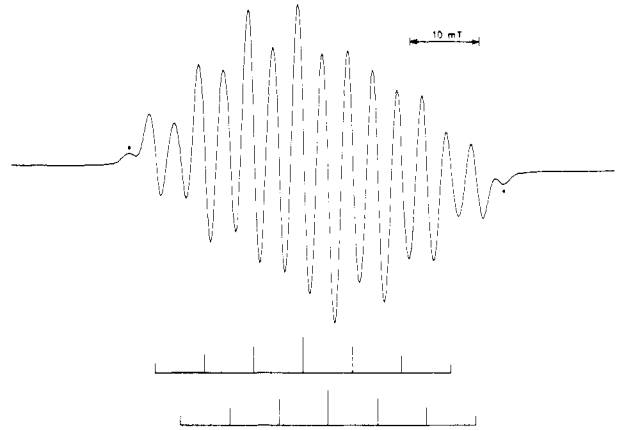


**Figure 6.** EPR spectrum with magnetic field in an arbitrary orientation, showing hyperfine splitting with two copper nuclei (indicated below the spectrum) and zero-field splitting. Satellite lines which are attributed to interpair exchange interactions are marked with dots.

**C. EPR Measurements.** In spite of the fact that the crystal is magnetically concentrated, no exchange narrowing was

(33) Bleaney, B.; Bowers, K. D. *Proc. R. Soc. London, Ser. A* **1952**, *214*, 451.

(34) Kolthoff, I. M.; Elving, P. J. *Treatise Anal. Chem. Part 1* **1963**, *4*.

**Table VII.** Experimental and Calculated Principal Values of g, Copper Hyperfine, and Zero-Field Splitting Tensors ($10^{-4}$ $cm^{-1}$) and Directions of Principal Axes Relative to Crystallographic Axes

| exptl | | | | | | calcd | | | | exptl[f] | |
|---|---|---|---|---|---|---|---|---|---|---|---|
| | principal values | directions (deg) a | b | c | | principal values | directions (deg) a | b | c | | principal values |
| | | | | | $x$[a] | | 93.2 | 76.3 | 158.7 | | |
| | | | | | $y$ | | 93.4 | 13.0 | 80.7 | | |
| | | | | | $z$ | | 174.0 | 95.1 | 73.5 | | |
| $g_\perp$ | 2.024 | | | | $g_1$[b] | 2.026 | 93.9 | 62.1 | 149.8 | $g_1$ | 2.023 |
| | | | | | $g_2$ | 2.027 | 90.9 | 27.3 | 67.9 | $g_2$ | 2.026 |
| $g_\parallel$ | 2.090 | 174 | 95 | 71 | $g_3$ | 2.110 | 174.6 | 93.7 | 71.9 | $g_3$ | 2.086 |
| $A_\perp - A_{av}$ | +37 | | | | $A_1 - A_{av}$[b] | +28.5, 38.9[e] | 92.1 | 107.1 | 151.4 | $A_1$ | 41.0 |
| | | | | | $A_2 - A_{av}$ | +28.1, 38.8 | 93.5 | 16.2 | 109.9 | $A_2$ | 41.0 |
| $A_\parallel - A_{av}$ | −74 | 174 | 95 | 72 | $A_3 - A_{av}$ | −56.6, −77.7 | 174.4 | 93.8 | 71.8 | $A_3$ | −82.0 |
| $A_{av}$ | −68.4 | | | | $A_{av}$ | +16.7 | | | | $A_{av}$ | −80.0 |
| $D_1$ | ∓22.4 | 67 | 61 | 53 | $D_1$[c] | +22.5 | 61.5 | 61.4 | 58.8 | | |
| $D_2$ | ∓24.9 | 31 | 121 | 109 | $D_2$ | +23.5 | 37.7 | 123.7 | 111.9 | | |
| $D_3$ | ±47.3 | 109 | 135 | 43 | $D_3$ | −46.0 | 111.6 | 132.3 | 39.3 | | |
| | | | | | $D_\perp$[d] | +23.0 | | | | | |
| | | | | | $D_\parallel$ | −46.0 | 104.2 | 131.6 | 36.8 | | |

[a] Directions of molecular axes. [b] Calculated with results of extended Hückel MO calculations. [c] Point dipole calculation, based upon the spin densities from extended Hückel MO calculations. [d] Point dipole calculation with spins located on the copper atoms. [e] First-order, dipole–dipole interaction only. [f] Experimental values from ref 2 of planar $[Cu(mnt)_2]^{2-}$ anion, diamagnetically diluted in the corresponding Ni(II) complex.

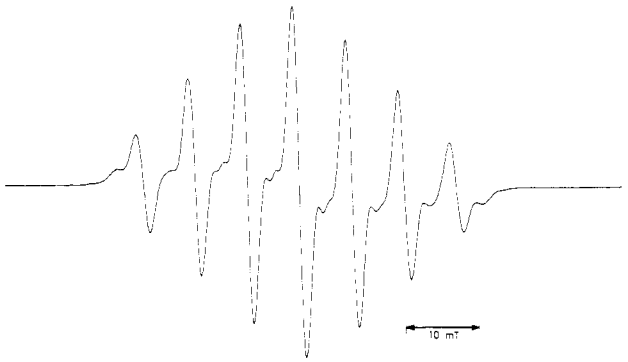


**Figure 7.** EPR spectrum with the magnetic field in an orientation such that the zero-field splitting is zero. The spectrum shows the coupling with two copper nuclei and the satellite lines.

observed in the EPR spectra. Two typical spectra are shown in Figures 6 and 7. The main lines, which are indicated below the spectrum in Figure 6, can be interpreted as being due to an electronic triplet state which arises from the exchange interaction between the two unpaired electrons in a pair of $[Cu(mnt)_2]^{2-}$ anions. The results of the previous section prove that the singlet state is the ground state, with the triplet state 5.2 $cm^{-1}$ above it. The satellite lines are thought to arise from interpair exchange and dipole–dipole interactions. A detailed explanation for their occurrence will be given in a forthcoming paper. The expected $\Delta M_s = 2$ transition could only be observed with the microwave field at an angle of 45° with the static field. The intensity was in the order of 1% of the intensity of the $\Delta M_s = 1$ transitions, in accord with calculated transition probabilities.

The main lines were described with the spin Hamiltonian

$$\mathcal{H}_S = \mu_B \vec{B}\cdot\boldsymbol{g}\cdot\vec{S} + \vec{S}\cdot\boldsymbol{A}\cdot(\vec{I}_1 + \vec{I}_2) + \vec{S}\cdot\boldsymbol{D}\cdot\vec{S} \qquad (3)$$

where $\vec{S} = 1$, $\vec{I}_1 = \vec{I}_2 = {}^3/_2$ are the spins of the copper nuclei, and all other symbols have their usual meaning. The data were analyzed with the computer program GAPLSD,[35] which is based on a strong field approximation for the various tensors. The resulting principal values of the tensors are listed in Table VII together with the direction angles of the principal axes, relative to the crystallographic axes. For comparison, the direction angles of the molecular axes $x$, $y$, and $z$ are given as well. The $z$ axis is along the normal to the least-squares plane through the copper and sulfur atoms of a $[Cu(mnt)_2]^{2-}$ monomer. The $x$ and $y$ axes are along the other two approximately twofold axes of the anion, with $x$ pointing from Cu to a point in between C(1) and C(2). So that a comparison with $[Cu(mnt)_2]^{2-}$ in a spin-doublet state could be facilitated, the listed copper hyperfine splitting has been multiplied by a factor of 2 (because $A$(triplet):$A$(doublet) = 1:2). Within experimental error, the $\boldsymbol{g}$ and copper hyperfine tensors are axially symmetric and have coinciding principal axes along the $z$ axis of the molecules. The largest zero-field splitting deviates only a few degrees from the Cu–Cu direction in the dimer.

So that more insight into the difference between the bonding properties of the anion in its "normal" planar geometry and in the current twisted one could be obtained, extending Hückel MO calculations were performed on both structures. The values for the empirical parameters and the basis set were taken from the calculations on bis(dithiocarbamato)copper(II).[36,37]

The symmetry of the planar anion is nearly $D_{2h}$. Then the MO of the unpaired electron has $B_{1g}$ symmetry and consists of the $3d_{xy}$ orbital of copper and hybrids of 3s, $3p_x$, and $3p_y$ orbitals of the sulfur atoms. The bonding is strongly covalent, as could be concluded from single-crystal EPR measurements on $(n\text{-}Bu_4N)_2[Cu(mnt)_2]$, diamagnetically diluted in the corresponding Ni(II) chelate.[2,38] Upon twisting of the ligands, the symmetry of the molecule is lowered to approximately $D_2$, and according to the extended Hückel results, the MO of the unpaired electron has $B_1$ symmetry. In this representation, the above mentioned atomic orbitals are mixed with the $p_z$ orbitals of copper and sulfur. This mixing has a direct effect on the copper hyperfine splitting: if the coefficients of $3d_{xy}$ and $4p_z$ in this MO are $\alpha$ and $\beta$, the first-order hyperfine splitting (hfs)[39] due to the spin densities in these orbitals are related as

$$A(3d_{xy}):A(4p_z) = -5\alpha^2\langle r^{-3}\rangle_{3d}:7\beta^2\langle r^{-3}\rangle_{4p} \approx -2\alpha^2:\beta^2$$

(35) Keijzers, C. P.; Paulussen, G. F. M.; de Boer, E. *Mol. Phys.* **1975**, *29*, 973.
(36) Keijzers, C. P., Ph.D. Thesis, University of Nijmegen, 1974.
(37) Keijzers, C. P.; de Boer, E. *Mol. Phys.*, **1975**, *29*, 1007.
(38) Kirmse, R.; Stach, J.; Dietzsch, W.; Hoyer, E. *Inorg. Chim. Acta* **1978**, *26*, L53.
(39) Keijzers, C. P.; de Boer, E., *J. Chem. Phys.* **1972**, *57*, 1277.

Table VIII. Symmetries in $D_2$, Occupation Numbers, Energies, and Most Important LCAO Coefficients of Cu, S(1), and S(4) Orbitals in the Highest Occupied and Lowest Unoccupied MO's

| orbital | symmetry in $D_2$ | no. of e | $E$, eV | orbitals of Cu | orbitals of S(1) | orbitals of S(4) |
|---|---|---|---|---|---|---|
| 47 | $A - B_3$ | 0 | −6.05 | | | $+0.31z + 0.15y$ |
| 46 | $A + B_3$ | 0 | −6.13 | | $+0.31z - 0.11y$ | |
| 45 | $B_1$ | 1 | −7.02 | $0.68xy + 0.26z$ | $-0.28z + 0.23x$ | $-0.30z - 0.22x$ |
| 44 | $B_2$ | 2 | −8.91 | $0.59xz$ | $+0.31z - 0.23y$ | $-0.30z - 0.26y$ |
| 43 | $B_3$ | 2 | −10.12 | $0.89yz$ | $+0.14y$ | $+0.14y$ |
| 42 | A | 2 | −10.16 | $0.45z^2 - 0.75x^2 - y^2$ | $-0.22y$ | $+0.23y$ |
| 41 | A | 2 | −10.35 | $0.48z^2 + 0.17x^2 - y^2$ | $-0.31z + 0.21y$ | $-0.29z - 0.22y$ |
| 40 | A | 2 | −10.40 | $0.64z^2 + 0.51x^2 - y^2$ | $0.05z - 0.11y$ | $0.07z + 0.09y$ |
| 39 | $B_2$ | 2 | −10.73 | $0.57xz$ | $-0.32z - 0.13y$ | $0.31z - 0.12y$ |

where the expectation values of $r^{-3}$ as calculated from radial atomic wave functions[40] are substituted. Thus, these contributions counteract each other, and therefore, twisting the ligands should result in a lowering of the anisotropic part of the copper hfs, even if the net spin density on copper ($\alpha^2 + \beta^2$) remains constant, as can be concluded from the extended Hückel calculation. This effect is clearly reflected in the experimental results (Table VII: the hfs's of the twisted complex are 10% smaller than those of the planar one. Also the expected lowering of the average hfs is reflected in the experimental values. The reason is that the main contribution to the Fermi-contact interaction is due to spin polarization of inner core s electrons. It is to be expected that 4p electrons have a smaller polarizing effect than 3d electrons; therefore, a decrease of the symmetry to $D_2$ results in a smaller (in absolute value) contact interaction. The effect on the **g** tensor is hard to assess with symmetry arguments only. Since the spin–orbit coupling of the copper 4p orbitals is as large as the coupling of the 3d orbitals, it is to be expected that the main effects on the **g** tensor will arise via changes in excited-state energies, which can hardly be predicted.

Table VIII lists the symmetries, energies, and most important LCAO coefficients of Cu, S(1), and S(4) in the highest occupied and lowest unoccupied MO's. The highest occupied ones all have metal 3d character but are highly delocalized. The lowest unoccupied MO's are localized on the ligands. The spin density on copper is about 0.5, the remaining 0.5 is localized on the sulfur atoms. As mentioned above, the lowering of the symmetry resulted in a mixing of the $p_z$ orbitals of copper and sulfur into the MO of the unpaired electron. With these extended Hückel results, the EPR parameters were calculated.

The calculated **g** tensor (Table VII) has its principal axes along the measured ones. Also the $g_\perp$ values are in agreement with experiment, but $g_\parallel$ is too large by 0.02. This is caused by the excitation energies of the MO's with $A$ symmetry ($d_{z^2}$, $d_{x^2-y^2}$), which are apparently too small. These small calculated excitation energies also have a large effect on the second-order contribution[39] to the hfs of copper. As a result, this spoils the agreement of the dipolar first-order interaction with experiment (Table VII) and introduces a large positive isotropic term.

The zero-field splitting tensor was computed with a nondelocalized electron spin and with the calculated spin densities of all atoms. Both tensors are only marginally different and agree very closely with the experimental one.

The calculated hfs's of sulfur are not listed in the table. From the calculations, they are expected to be $A_\perp \approx -3.8$, $A_\parallel \approx +7.6$, and $A_{av} \approx +3.9\ 10^{-4}$ cm$^{-1}$, hence total values of $A_\perp \approx 0$ and $A_\parallel \approx 11.5\ 10^{-4}$ cm$^{-1}$, appreciably smaller than the splittings in the planar complex.[38]

Concluding one may say that the combined susceptibility and EPR measurements, together with the semiempirical MO calculations, give a good insight in the electronic structure of the $[Cu(mnt)_2]^{2-}$ anions and in the effect on it of ligand twisting and pair formation. We expect that additional analysis of the satellite lines in the EPR spectra will yield information about interpair interactions, as will be discussed in a forthcoming paper.

**Acknowledgment.** We wish to express our gratitude to Dr. Jan Noordik for collecting the crystallographic data and for determining the orientation of the crystal axes of the crystal that was used for the EPR experiments. We wish to thank Professor E. de Boer for critical reading of the manuscript. H.M.D. was supported by the Netherlands Foundation for Chemical Research (SON) and part of this work was supported by the "Stichting voor Fundamenteel Onderzoek der Materie" (FOM), both with financial aid from the Netherlands Organisation of Pure Research (ZWO).

**Registry No.** $[Cu(mnt)_2]^{2-}[MB^+]_2$·(acetone), 77481-61-9; $[Cu(mnt)_2]^{2-}[MB^+]_2$, 77481-60-8.

**Supplementary Material Available:** Listings of hydrogen atom coordinates (Table II), anisotropic temperature factors of the nonhydrogen atoms (Table V), and observed and calculated structure factors (28 pages). Ordering information is given on any current masthead page.

(40) Bancroft, G. M. "Mössbauer Spectroscopy"; McGraw-Hill: London, 1973; p 27.
(41) Clementi, E.; Roetti, C., *At. Data Nucl. Data Tables* **1974**, *14*, 177.